J Solid State Electrochem (2015) 19:201–210
DOI 10.1007/s10008-014-2582-0

ORIGINAL PAPER

The effect of pH and selenization on the properties of $CuInSe_2$ thin films prepared by electrodeposition technique for device applications

Ashwini B. Rohom · Priyanka U. Londhe · N. B. Chaure

Received: 2 June 2014 / Revised: 10 July 2014 / Accepted: 11 July 2014 / Published online: 1 August 2014

Abstract We have synthesized $CuInSe_2$ (CIS) thin films from an aqueous electrolyte by potentiostatic electrochemical technique at room temperature. The effects of pH and selenization on the properties of CIS layer have been thoroughly investigated. The studies were carried out on the samples prepared in as-prepared bath with pH 2.5 and later adjusted to 1.2. Cyclic voltammetry (CV) was studied at slow scan rate to optimize the deposition parameters. The prepared thin films were selenized in a tubular furnace at 400 °C for 20 min in selenium atmosphere. Structural, optical, compositional, morphological, and electrical properties were studied with the help of X-ray diffractometer, Uv-vis absorption spectroscopy, energy dispersive X-ray analysis (EDAX), scanning electron microscopy (SEM), and current–voltage (*I–V*) measurements. The prominent reflections (112), (204/220), and (312/116) of tetragonal CIS have been exhibited for all as-deposited and selenized samples. The energy band gap of the selenized CIS thin film was found to be ~1.03 eV. Granular, uniform, and densely packed surface morphology was observed for as-deposited and selenized samples electrodeposited at −0.6 and −0.8 V versus Ag/AgCl for the pH of bath 1.2 and 2.5, respectively. EDAX result reveals the stoichiometric CIS films can be electrodeposited at −0.6 and −0.8 V with pH of the bath 1.2 and 2.5, respectively. The ideality factor (η) deducted from *I–V* measurements was found to be reduced from 1.6 to 1.3 and 1.9 to 1.2 after selenization of samples grown at −0.6 and −0.8 V, respectively, revealing the formation of ideal diode due to elimination of surface leakage current. Photoelectrochemical (PEC) measurement confirms the growth of p-type CIS thin film.

A. B. Rohom · P. U. Londhe · N. B. Chaure (✉)
Electrochemical Laboratory, Department of Physics, University of Pune, Pune 411007, India
e-mail: n.chaure@physics.unipune.ac.in

Keywords $CuInSe_2$ films · Electrodeposition · Photoelectrochemical measurement · Cyclic voltammetry · Effect of pH

Introduction

The chalcopyrite semiconductors such as $CuInSe_2$ (CIS), $CuInGaSe_2$ (CIGS), and $CuInTe_2$ have attracted significant interest as a photo-absorbing material of thin film solar cells because of high absorptivity (>10^5 cm^{-1}) and physical and chemical stability against photo-degradation [1–3]. CIS has a direct band gap tunable from 1.04 to 1.68 eV upon addition of gallium (Ga) and sulfur (S), which is within the maximum solar absorption region. These properties of CIS-based materials make possible to achieve 20.3 % [2] and 15.7 % (http://www.miasole.com) power conversion efficiency for a laboratory cell and module. Several methods have been investigated for the deposition of CIS thin films such as co-evaporation [4], sputtering [5], spray pyrolysis [6], molecular beam epitaxy [7], stacking elemental layers [8], flash evaporation [9], pulsed laser deposition [10], and electrodeposition [11] etc. The high-efficiency solar cells have been prepared by vacuum-based co-evaporation methods; however, it has technical challenges in terms of scale up because of non-uniform evaporation of metal precursors at high temperature over large area and requires expensive equipment. These issues can be overcome by non-vacuum electrodeposition technique, which has several advantages, such as low production cost, utilization of over 95 % materials, to deposit over large areas, and non-planer substrates. Moreover, by electrodeposition, much higher deposition rate can be achieved with controlled thickness of the film, particle size, and stoichiometry [12–14].

Three different processes are employed to deposit CIS thin films by three-electrode electrodeposition technique: one-step electrodeposition [15, 16] in which all elements can be co-

electrodeposited at a particular potential to get stoichiometric layers, the selenization of Cu–In alloys formed by electrodeposition [17], and the pulse plating electrodeposition where the cathode is modulated by the pulse potential [18]. CIS can also be electrodeposited by two-electrode systems [19]. In order to electrodeposit stoichiometric CIGS (Cu, 25 %; In, 12.5 %; Ga, 12.5 %; and Se, 50 %), it is important to use appropriate additives/supporting chemicals, complexing agents along with pH of the solution due to the wide differences in the equilibrium potentials of Cu, Se, In, and Ga. Alternatively, more In and Ga can be incorporated in CIGS by electrodepositing at higher negative potentials, −0.9 V and above, versus Ag/AgCl. However, the hydrogen evolution reaction limits the use of higher cathodic potentials due to powdery, non-uniform, and patchy deposition. The pH of electrolyte can play an important role to reduce the electrodeposition potential due to the availability of more OH^- ions, which can either form the complex with noble elements or reduce the open circuit potentials (OCP). Calixto et al. [20] reported the electrodeposition of nearly stoichiometric CIS thin films for different pH values of the bath. Recently, Bao-Ping et al. [21] have reported the pH value of the bath could regulate the stoichiometry of In and Ga.

In this paper, we report the electrodeposition of CIS thin films in an aqueous medium for different pH of the solution. The conditions to deposit stoichiometric and highly crystalline films are optimized for different electrodeposition potentials with the pH 1.2 and 2.5. Samples were characterized with a range of characterization techniques to study the crystal structure, optical band gap, grain growth, bulk composition, and conductivity type.

Experimental details

CIS thin films have been potentiostatically deposited by cathodic electrodeposition technique. Five-necked, custom-made, air-tight electrochemical cell was employed for the electrodeposition of CIS thin films. Fluorine-doped tin oxide (FTO)-coated glass substrates, Ag/AgCl, and graphite were used as working, reference, and counter electrodes, respectively. The electrolytic bath was made in an aqueous solution which consists of a matrix of 3–5 mM copper chloride ($CuCl_2$), 3–6 mM indium tri-chloride ($InCl_3$), and 3–8 mM selenous acid (H_2SeO_3). Lithium chloride (LiCl) was used as supporting electrolyte. The pH of the bath was adjusted using either HCl or NaOH to 1.2 and 2.5 at room temperature. The co-deposition potential of Cu, In, and Se was optimized by studying cyclic voltammetry (CV) for different pH of the bath. The cyclic voltammograms were recorded without stirring at room temperature with a scan rate 5 mV/s. The CIS thin films were electrodeposited in a plateau region −0.6 to −0.8 and −0.4 to −0.6 V (versus Ag/AgCl) observed from CV for the pH of the bath 2.5 and 1.2, respectively. Immediately after deposition, the samples were thoroughly rinsed in warm water and cleaned by pulling wet tissue paper on the surface of sample to remove the loosely bound particles. Subsequently, the films were dried in an open air and used for further characterizations. The CIS thin films were selenized in a homemade tubular selenization chamber at 400 °C for 20 min.

Chemicals

All the chemicals used for electrochemical synthesis of CIS were purchased from Sigma-Aldrich of purity at least 99.9 % and used as received. The commercially available FTO-coated glass substrates of sheet resistance 10–15 Ω/□ were purchased from Pilkington glass company, UK. The double-distilled deionized water was used as a solvent to dissolve the precursors of Cu, In, and Se.

Materials characterization

Cyclic voltammetric studies and the electrodeposition of CIS were carried out by using μ3AUT 70762 AUTOLAB potentiostat/galvanostat. The structural properties were studied by means of X-ray diffraction (XRD), model Bruker D8 ADVANCE diffractometer with Cu Kα anode of wavelength 0.154 nm. Optical absorption measurements were carried out by JASCO UV-Vis-NIR spectrometer. Surface morphology was studied with the help of JEOL JSM 6360 A scanning electron microscope with an operating voltage 20 kV. The elemental atomic percentage concentration of the layer was obtained by energy dispersive X-ray analysis technique equipped with the above scanning electron microscopy (SEM) unit. The potentiostat, SP 300, Bio-Logic, equipped with two probe measurement set-up was employed to study the electrical (*I–V*) properties. The conductivity type of p-type silicon, n-type silicon, and annealed CIS films was studied by photoelectrochemical (PEC) analysis. Three-electrode geometry was employed for PEC studies with graphite and Ag/AgCl as counter and reference electrodes, respectively, in 1 M KCl solution. A white light source with an intensity approximately 100 mW/cm^2 was used to illuminate the sample with applied potential of −10 mV for photoelectrochemical study.

Results and discussion

The co-deposition potential for Cu, In, and Se was optimized by cyclic voltammetry at room temperature without agitation. Typical cyclic voltammograms recorded in the presence of Cu, In, and Se ionic species with pH 1.2 and 2.5 are shown in

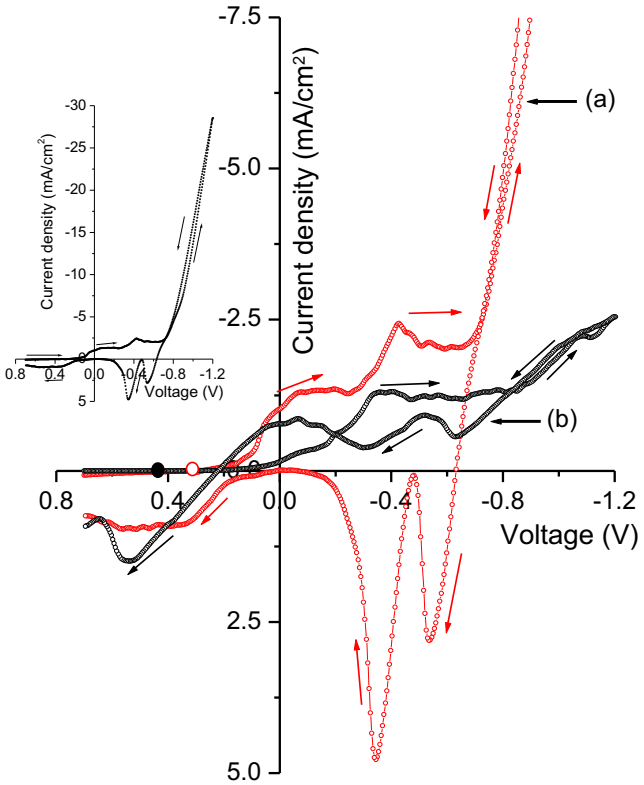

Fig. 1 Typical cyclic voltammograms recorded in the matrix of Cu, In, and Se precursors in an aqueous bath with pH 1.2 (**a**) and 2.5 (**b**) at room temperature without agitation. The scan rate was 5 mV/s. *Inset* shows the CV recorded in the bath with pH 1.2. The *circles*, *open* and *solid*, demonstrate the open circuit potentials, +0.33 and +0.42 V, measured prior to beginning the CV in pH 1.2 and 2.5, respectively

Fig. 1a, b, respectively. Inset in Fig. 1 shows the complete CV recorded with the pH of the bath 1.2. A gradual shift in onset potential for the reduction of Se ions, from +1.0 to ~0.0 V, has been observed for pH 1.2 and 2.5, respectively, which could be due to the availability of large number of hydroxide (OH^-) ions at higher pH and/or shift in the open circuit potentials (OCP). The values of OCP, +0.33 and +0.42 V, were measured for the CIS bath with pH 1.2 and 2.5, respectively This indicates that the reduction of electroactive species begins at higher cathodic potential for pH 2.5 as compared to lower pH (1.2) of the bath. A higher cathodic current density was measured for 1.2 pH of the bath. Initially, at lower cathodic potentials up to −0.3 V, the features noticed are assigned to the reduction of Cu and Se by the following charge-transfer reactions:

$$Cu^{2+} + 2e^- \rightarrow Cu \qquad E_o = +0.34\,V \text{ versus SHE} \qquad (1)$$

$$H_2SeO_3 + 4e^- + 4H^+ \rightarrow Se + H_2O \quad E_o = +0.74\,V \text{ versus SHE} \qquad (2)$$

Metallic In is proposed to be electrodeposited in the plateau region observed in CVs by the following charge transfer reaction:

$$In^{3+} + 3e^- \rightarrow In \qquad E_o = -0.34\,V \text{ versus SHE} \qquad (3)$$

The electrodeposition of CIS takes place as per following reaction:

$$Cu^{2+} + In^{3+} + 2SeO_3^{2-} + 9e^- + 12H^+ \rightarrow CuInSe_2 + 6H_2O \qquad (4)$$

A plateau region attributed at lower cathodic potentials (+0.1 to −0.3 V) for the lower pH of the bath (Fig. 1a) is proposed due to the reduction of Cu and Se ions, which favors the electrodeposition of secondary phases of Cu_xSe_y. A flat limiting current region, which is unaffected by the applied potential, was observed in the range −0.42 to −0.62 and −0.35 to −0.80 V for pH 1.2 and 2.5, respectively. This region is assigned the diffusion-controlled electrodeposition which could be suitable for the synthesis of polycrystalline and controlled stoichiometric CIS thin films. Furthermore, a steep rise in the cathodic current was also found to be shifted from about −0.80 to −0.65 V for pH 2.5 and 1.2 which could be due to the availability of more H^+ ions at lower pH of the bath. The sharp rise in the cathodic current observed at −0.80 and −0.65 V for pH 2.5 and 1.5 could be due to the hydrogen evolution as well as the metallic deposition of In. The shift, 0.15 V versus Ag/AgCl, observed in the hydrogen evolution reaction could be associated with the availability of more H^+ ions at lower pH of the bath. The effect of pH can be further understood by the factors dominated in an electrodeposition process, such as dissolution of the freshly deposited metal atoms on the substrate because of acidic electrolyte, formation and absorption of metal hydroxide on the electrode surface, and the anomalous electrodeposition of metals [22]. A lower pH value (films deposited at −0.6 V in 1.2 pH bath) favors the dissolution of freshly deposited metals and slows down the formation and absorption of metal hydroxide. The process is predominated by the first factor resulting in a higher In content in the films due to higher In^{3+} in the electrolyte. Higher pH values (films deposited at −0.6 V in 2.5 pH bath) favors the formation and absorption of metal hydroxide and slows down the dissolution of the freshly deposited metals, resulting in a lower In content because of the preferential absorption of indium oxide in the electrolyte. This indicates that the indium deposition can be suppressed due to the increase of pH (2.5), leading to a negative shift in indium deposition potential; therefore, the deposition potential of CIS has been shifted towards more cathodic potential (−0.8 V).

This indicates that the low pH of the bath may not be suitable to obtain the stoichiometric CIS thin films due to the hydrogen evolution at lower cathodic potential. It is also known that less hydrogen evolution is helpful to passivate the oxidation of precursor layer during the growth, whereas heavy hydrogen evolution prepares the amorphous, powdery, and patchy films with very rough surface. The stripping peaks related to In, Cu, and Se are observed in both CVs during the anodic scan around −0.60, −0.40, and +0.50 V, respectively.

The SEM images of CIS thin films electrodeposited at potential −0.4 and −0.6 V in an electrolytic bath having pH 1.2 are depicted in Fig. 2a, b, respectively. Uniform, densely packed, and compact surface morphology without voids can be clearly seen from the SEM micrographs. The sample deposited at −0.4 V exhibited a mixed granular and flake like morphology (Fig. 2a). The flakes seem to be uniform in size with random orientation. The samples prepared at −0.6 V were deposited large micron-size clusters due to agglomeration of small particles. The SEM images of CIS thin films electrodeposited at potentials −0.6 and −0.8 V in the bath of pH 2.5 are shown in Fig. 3a, b, respectively. The spherical grains of size ~1 μm is uniformly deposited all over the substrate at growth potential −0.6 V, whereas the powdery surface with tiny grains of size approximately 100 nm can be seen for the sample deposited at −0.8 V. Prior to recording of the SEM micrograph shown in Fig. 3b, the sample was cleaned by pulling wet tissue paper over the powdery surface and subsequently ultrasonicating for few minutes. Both CIS thin films were found to be deposited uniformly all over the surface without voids.

The elemental compositional analysis obtained by energy dispersive X-ray analysis (EDAX) for CIS thin films electrodeposited at various deposition potentials in the bath having pH 1.2 and 2.5 is summarized in Table 1. It was observed that the CIS thin films close to stoichiometry (25:25:50) are deposited at −0.6 and −0.8 V in the bath of pH values 1.2 and 2.5, respectively. We found that the lower deposition potentials, −0.4 and −0.6 V for pH 1.2 and 2.5, respectively, favor the electrodeposition of more Cu in the complex form. The pH and potential-dependent growth of ternary alloy $Cu_xIn_{1-x}Se_2$, binary compounds $Cu_xSe_y/In_xSe_y/In_xCu_y$, and metals have been discussed thoroughly by Pourbiax [23]. The electrodeposition potential for stoichiometric CIS thin films was found to be shifted towards higher cathodic potential as the pH of the bath increases. The stoichiometric CIS thin films are deposited

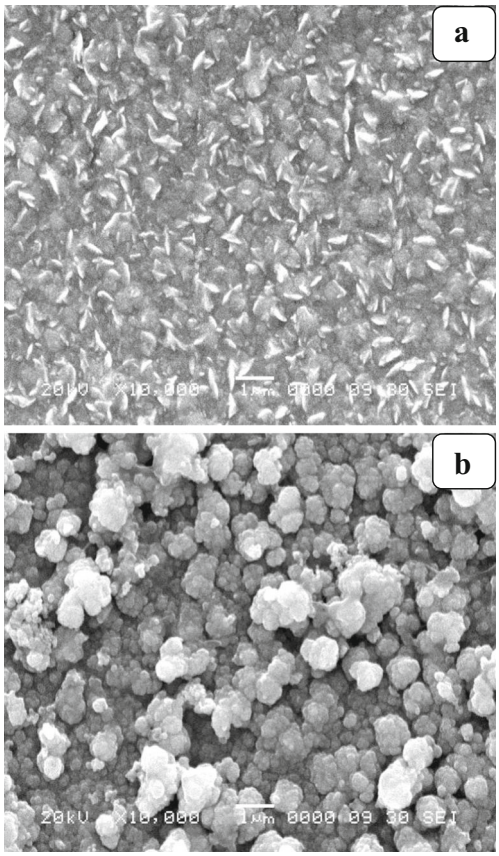

Fig. 2 SEM images of as-deposited CIS thin films electrodeposited at −0.4 V (**a**) and −0.6 V (**b**) with the pH of the bath 1.2

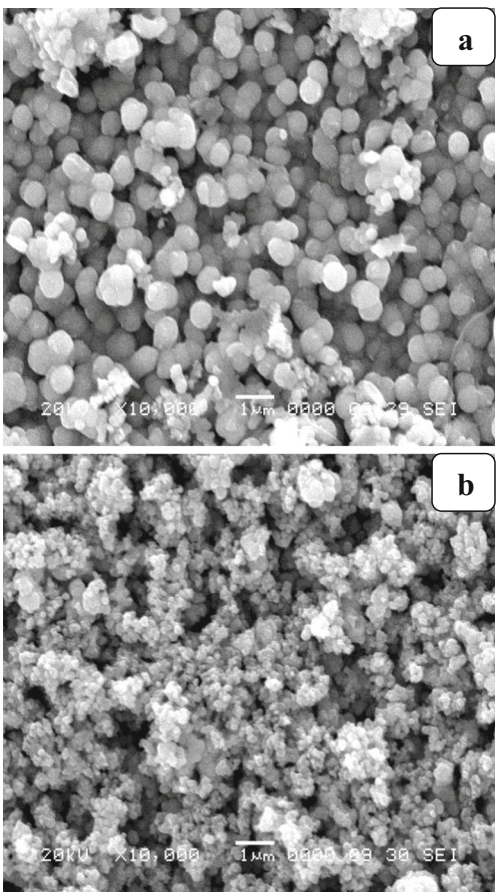

Fig. 3 SEM micrographs of as-deposited CIS thin films electrodeposited at −0.6 V (**a**) and −0.8 V (**b**) versus Ag/AgCl reference electrode in an electrolyte of pH 2.5

Table 1 A summary of the atomic percentage concentration of Cu, In, and Se obtained by EDAX for as-deposited CIS thin films deposited at different deposition potentials in the bath with pH 1.2 and 2.5

pH of the bath	Deposition potential (V)	Atomic concentration (%)		
		Cu	In	Se
1.2	−0.4	41.06	15.92	43.02
	−0.6	28.67	21.77	49.56
2.5	−0.6	47.78	15.45	36.77
	−0.8	29.76	25.08	45.14

at −0.6 and −0.8 V (versus Ag/AgCl) for the pH of the bath 1.2 and 2.5, respectively.

The stoichiometric films obtained at potentials −0.6 and −0.8 V from the solution having pH 1.2 and 2.5 were selenized in a homemade tubular selenization chamber. Selenization process was performed under selenium atmosphere with a controlled pressure at high temperature above 400 °C for 20 min. Here, we have used elemental Se vapors in a vacuum ~5×10^{-5} Torr. Figure 4 shows the SEM images of selenized CIS thin films electrodeposited at −0.6 and −0.8 V in the solution of pH 1.2 and 2.5, respectively. Selenization

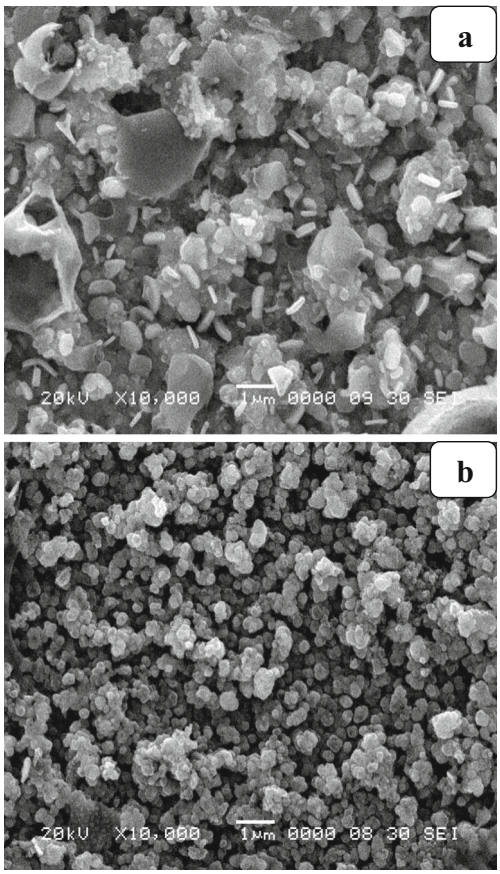

Fig. 4 SEM images of selenized CIS thin films electrodeposited at −0.6 V (**a**) and −0.8 V (**b**) in an electrolyte with pH 1.2 and 2.5, respectively

played a very important role to change the surface morphology significantly as well as to control the overall atomic percentage concentration of In, Cu, and Se. The enhancement in the particle size can be clearly seen in Fig. 4. The grain size can be further improved with the desired elemental composition suitable for high-efficiency solar cell by systematic work on the optimization of selenization temperature, ambient conditions, and the pressure of the selenium gas.

The elemental percentage concentration obtained for selenized CIS thin films electrodeposited at potentials −0.6 and −0.8 V in an electrolyte having pH 1.2 and 2.5 is summarized in Table 2. After selenization slightly, Cu-rich CIS layers are obtained. It has been reported that the Cu-rich CIS (p-type) absorber layer and a copper-deficient surface layer, which is generally known as ordered defect compounds, are required for high-efficiency solar cell [24]. It was further observed that the contents of Cu has been reduced, probably due to the incorporation of Se during the selenization procedure, while the In composition was reduced, may be due to the In loss mechanism by forming In_2Se compound. The values of Cu/In ratio 1.63 and 1.48 were calculated after selenization for CIS samples deposited at −0.6 and −0.8 V in the bath of pH 1.2 and 2.5, respectively. The excess Cu present in the CIS sample can be further reduced either by limiting the content of Cu during the growth process or etching the selenized CIS layer in the KCN solution [25].

As the stoichiometric CIS thin films are obtained at −0.6 and −0.8 V versus Ag/AgCl from the electrolyte having pH values 1.2 and 2.5, respectively, we, therefore, have reported herewith the structural, optical, morphological, compositional, and electrical properties of these films. Figures 5 and 6 show XRD patterns of as-deposited and selenized stoichiometric CIS thin films deposited at −0.6 and −0.8 V in the bath of pH 1.2 and 2.5, respectively. Three predominant reflections of the tetragonal structure of CIS corresponding to (112), (204/220), and (312/116) are attributed in all as-deposited and selenized samples without formation of secondary phases or metallic deposition. This peak matches very well with the JCPDS data card no. 35–1349. The reflections appeared from the FTO substrate is marked as solid circles (●). The enhancement in the crystallinity of the samples was studied by calculating the full width at half maxima (FWHM). The observed and standard values of 2θ, inter-planer distance d, and FWHM are summarized in Table 3. The values of FWHM are found to be decreased after selenization for all CIS peaks, indicating the enhancement in the degree of crystallinity, which could also correlate to the formation of larger clusters with selenization. Indeed, we have noticed the remarkable enhancement in the particle size after selenization, Fig. 4a, b. Furthermore, the FWHM calculated for CIS samples deposited at −0.6 V in the pH of the bath 1.2 is much smaller than that of the sample deposited at −0.8 V in the bath having pH 2.5, which is proposed due to the deposition of larger grains and the strain

Table 2 A summary of atomic percentage concentration of Cu, In, and Se in as-deposited and selenized CIS thin films deposited at −0.6 V in 1.2 pH and at −0.8 V in 2.5 pH bath obtained by EDAX analysis

pH of the bath	Deposition potential (V)	Atomic % concentration					
		Cu		In		Se	
		As-deposited	Selenized	As-deposited	Selenized	As-deposited	Selenized
1.2	−0.6	28.67	26.97	21.77	16.47	49.56	56.57
2.5	−0.8	29.76	28.41	25.08	19.16	45.14	52.43

developed between the substrate and precursor layer. Williamson–Hall (W–H) equation was employed to calculate the values of strain and crystallite size of the as-deposited and selenized CIS thin films. The FWHM can be expressed as a linear combination of the contributions from both strain and crystallite size through the equation given as follows [26].

$$\beta\cos\theta = \eta\sin\theta + \frac{\lambda}{t} \tag{5}$$

where, β is the average value of FWHM diffraction peaks, θ is the Bragg diffraction angle, λ is the wavelength of Cu Kα line (λ=0.154 nm), η is the strain, and t is the average crystallite size.

The values of the strain are calculated from the slope of the plot of $\beta\cos\theta$ versus $\sin\theta$, whereas the inverse of the intercept gives average crystallite size. Figure 7 depicts the plot of $\beta\cos\theta$ versus $\sin\theta$ for as-deposited and selenized CIS thin films deposited at −0.6 and −0.8 V in the bath with pH 1.2 and 2.5, respectively. It was observed that the crystallite size calculated for the sample deposited at −0.6 V in the pH of the bath 1.2 is larger than that of the sample deposited at −0.8 V in the pH of the bath 2.5. The values of the crystallite size and strain calculated by the Hall equation are summarized in Table 4. The positive value of the strain indicates the presence of effective tensile strain present in a crystal lattice [27]. The values of the strain, 1.88 and 1.51 for as-deposited and 2.50 and 1.83 for selenized CIS thin films electrodeposited at −0.6 and −0.8 V with pH of the bath 1.2 and 2.5, respectively, were calculated. The strain was found to be increased after selenization could be due to the enhancement in the crystallite

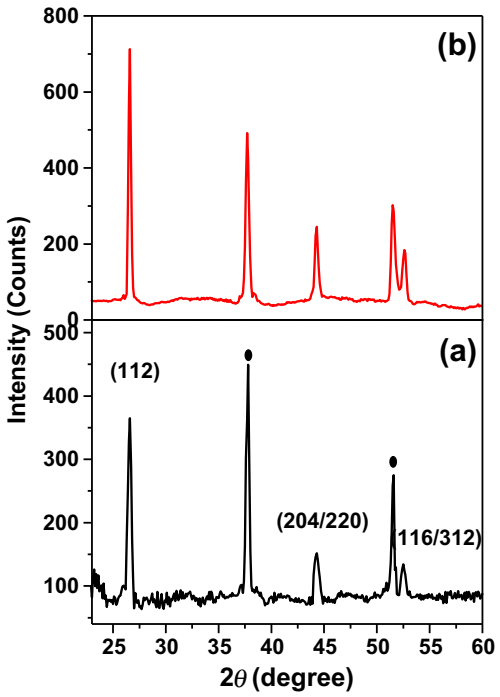

Fig. 5 X-ray diffraction pattern of as-deposited (**a**) and selenized (**b**) CIS thin films electrodeposited at −0.6 V in an electrolyte with pH 1.2. *Solid circles* marked in the figure represent the peaks attributed from FTO substrate

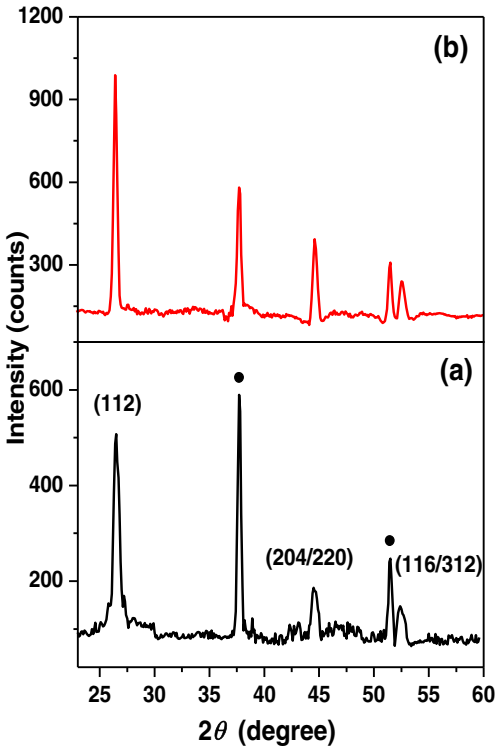

Fig. 6 X-ray diffraction pattern of as-deposited (**a**) and selenized (**b**) CIS thin films electrodeposited at −0.8 V from aqueous solution with pH 2.5. *Solid circles* marked in the figure represent the peaks attributed from FTO substrate

Table 3 A summary of the calculated values of FWHM, inter-planner distance *d* values of diffraction peak obtained from XRD results for the as-deposited and selenized CIS sample deposited at −0.6 V in 1.2 pH bath and at −0.8 V in 2.5 pH bath

pH of the bath	Deposition potential (V)	2θ (deg)			d (Å)			FWHM (deg)		Miller Indices
		Observed		Standard	Observed		Standard	Observed		
		As-deposited	Selenized		As-deposited	Selenized		As-deposited	Selenized	
1.2	−0.6	26.57	26.62	26.62	3.352	3.345	3.345	0.307	0.240	(111)
		44.27	44.30	44.28	2.043	2.043	2.043	0.350	0.291	(204/220)
		52.41	52.50	52.41	1.744	1.741	1.744	0.394	0.336	(116/312)
2.5	−0.8	26.40	26.49	26.62	3.372	3.360	3.345	0.492	0.331	(111)
		44.45	44.49	44.28	2.035	2.034	2.043	0.539	0.378	(204/220)
		52.36	52.51	52.41	1.745	1.740	1.744	0.611	0.438	(116/312)

size and/or recrystallization of CIS grains. The average crystallite size have also been calculated from the Debye Scherrer formula given as follows [28]:

$$t = \frac{0.9\lambda}{\beta\cos\theta} \tag{6}$$

where, β is the FWHM of diffraction peak, θ is the Bragg angle, λ is the wavelength of Cu Kα line, and t is the average grain size. The values of average crystalline size estimated by the Scherrer classical formula are given in Table 4. We have found that the values of crystallite size calculated by the Scherrer formula showed the similar trend observed by the Williamson–Hall equation.

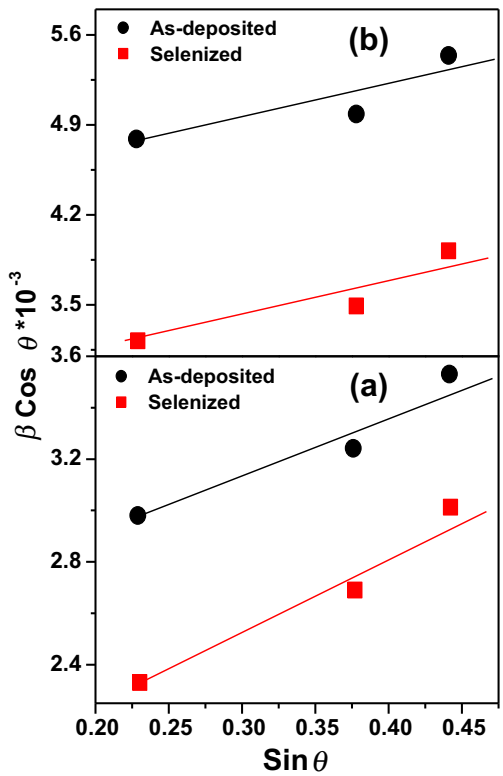

Fig. 7 Plot $\beta\cos\theta$ versus $\sin\theta$ for as-deposited and selenized CIS thin films electrodeposited at −0.6 V (**a**) and −0.8 V (**b**) in the bath with pH 1.2 and 2.5, respectively

Figure 8 shows a plot of $(\alpha h\nu)^2$ versus $(h\nu)$ for as-deposited and selenized CIS thin films electrodeposited at −0.6 and −0.8 V from the bath of pH 1.2 and 2.5, respectively. The band gap was found to be 1.13 to 1.16 eV for as-deposited and 1.03 to 1.06 eV for selenized CIS thin films electrodeposited at −0.6 and −0.8 V, respectively. These estimated values of the energy band gap are in good agreement with the literature values [25]. After selenization, the band gap of CIS was found to be decreased, which could be due to increase in particle size or re-crystallization of particles.

Figure 9 shows the current density–voltage (*J*–*V*) characteristics of the as-deposited and selenized CIS films deposited at −0.6 and −0.8 V in the solution having pH 1.2 and 2.5, respectively. Au metal contact with diameter 2 mm was made on FTO/CIS thin films by thermal evaporation technique. Schottky behavior was observed for both as-deposited and selenized samples; however, the diode curve close to the ideal one was observed after selenization. No noticeable change was observed in the forward current density for as-deposited and selenized samples, whereas the very less reverse current was measured for selenized CIS samples. This could be due to the recrystallization of the material which helps to prevent the flow of leakage current. The semilogarithmic graph of ln(*I*) against the applied voltage is depicted in Fig. 10. The values of the ideality factor (η) are calculated from the slope of the straight line region in the range 0.04 to 0.17 V of the forward bias *J*–*V* characteristics by using the following equation [29]:

$$\eta = \frac{q}{kT}\frac{\mathrm{d}V}{\mathrm{d}(\ln I)} \tag{7}$$

where q is the charge of electron, V is the applied voltage, η is the ideality factor, k is the Boltzmann constant, T is the temperature, and I is the diode current.

Table 4 The crystallite size and strain calculated by the Hall equation and Scherrer formula

pH of the bath	Deposition potential (V)	Crystallite size (nm) from the Debye Scherer formula		Williamson–Hall analysis					
				Crystallite size (nm)		Types of strain (tensile (T) or compressive (C))		Strain × 10^{-3}	
		As-deposited	Selenized	As-deposited	Selenized	As-deposited	Selenized	As-deposited	Selenized
1.2	−0.6	23.85	29.10	27.30	31.72	T	T	1.88	2.50
2.5	−0.8	15.50	22.13	17.09	24.40	T	T	1.51	1.83

The values of ideality factor 1.6 and 1.3 were calculated for the as-deposited and selenized CIS thin films electrodeposited at −0.6 V for the pH of bath 1.2, whereas 1.9 and 1.2 were obtained for the sample deposited at −0.8 V in the bath with pH 2.5. For an ideal diode, the ideality factor has to be unity. The value of ideality factor measured greater than unity could be due to the Fermi level pinning at interface [30] or relatively large voltage drops at the interface region. The values of the ideality factor decreases after selenization, indicating the formation of ideal diode due to increase in shunt resistance.

Figure 11 presents the photocurrent–time curves recorded by photoelectrochemical (PEC) test for standard n-type, standard p-type, and selenized CIS thin films (deposited at −0.6 and −0.8 V in 1.2 and 2.5 pH bath) in 1 M KCl solution under chopped illumination at −10 mV versus Ag/AgCl. In the photoelectrochemical process, the photocurrent originated from the minority carriers; therefore, the direction of observed photocurrent can give an idea of the type of majority charge carries. We have used a standard p-type and n-type silicon samples of resistivity, 0.05 Ω cm, as a reference.

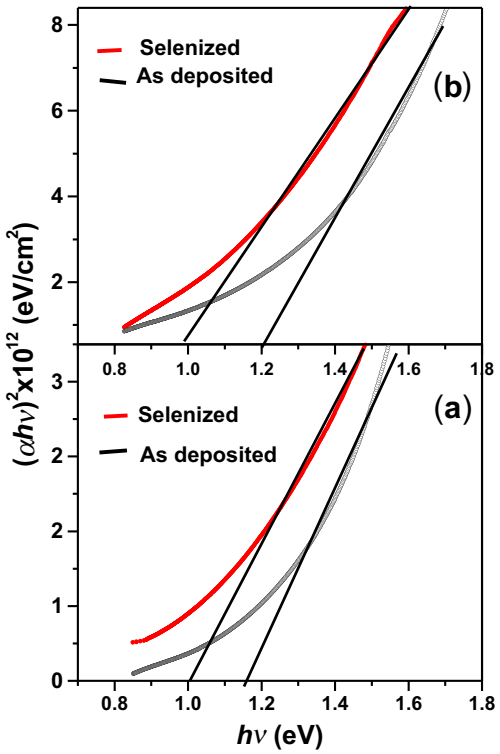

Fig. 8 Optical absorption spectra, $(\alpha h\nu)^2$ versus $(h\nu)$ of as-deposited and selenized CIS thin films deposited at −0.6 V (**a**) and −0.8 V (**b**) (vs Ag/AgCl reference) in the bath with pH values 1.2 and 2.5, respectively

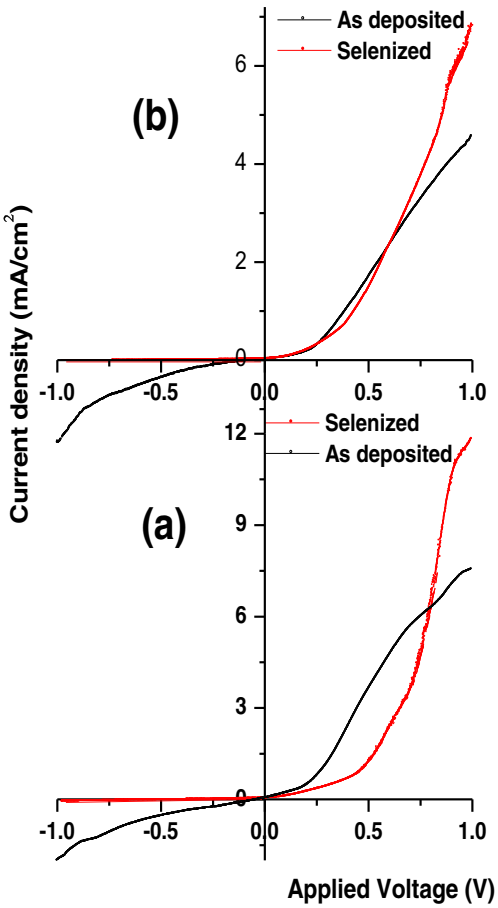

Fig. 9 Current density–voltage (J–V) characteristics of as-deposited and selenized CIS thin films electrodeposited at **a** −0.6 V and **b** −0.8 V with pH 1.2 and 2.5, respectively

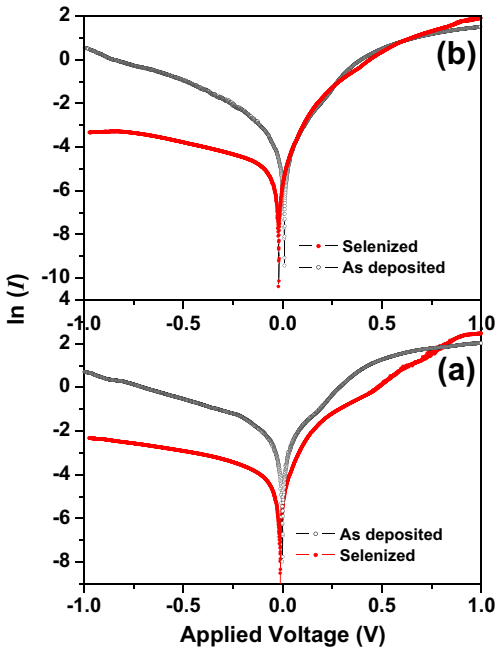

Fig. 10 Semilogarithmic graphs of ln(*I*) versus applied voltage of as-deposited and selenized CIS thin films deposited at −0.6 V (**a**) and −0.8 V (**b**) in an electrolyte with pH 1.2 and 2.5, respectively

The photocurrent measured for n-type sample upon illumination was found to be increased towards the positive direction (Fig. 11a), whereas the enhancement in the photocurrent was noticed along the negative direction for p-type Si sample (Fig. 11b). The photocurrent measured for selenized CIS thin films electrodeposited at −0.6 V (Fig. 11c) and −0.8 V (Fig. 11d) was found to be increased towards the negative direction under illumination of white light, indicating the p-type conductivity. The sharp edges observed with switching the light ON and OFF indicate that the CIS samples are defect-free and could be suitable for the development of high-efficiency solar cells without obstacle to the flow of charge carries generated upon illumination.

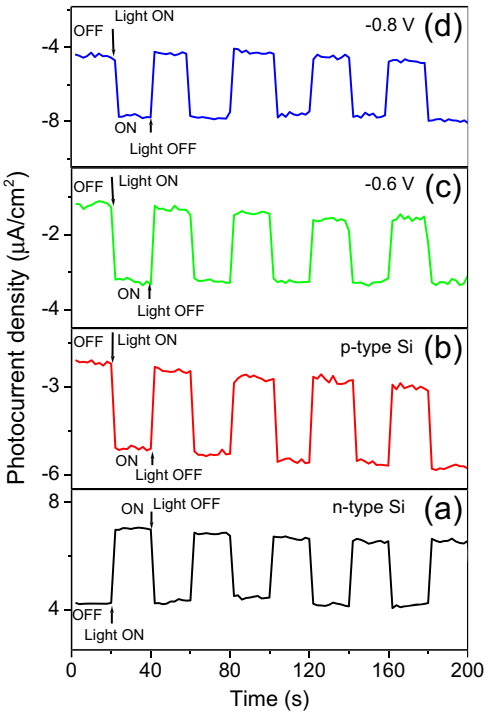

Fig. 11 Photoresponse curves, photocurrent density versus time for standard n-type silicon (**a**), p-type silicon (**b**), selenized CIS thin films deposited at −0.6 V (**c**) and −0.8 V (**d**) in an electrolyte with pH 1.2 and 2.5, respectively

Conclusions

In summary, we have successfully electrodeposited polycrystalline CIS thin films by one-step electrodepostion technique from an aqueous bath with pH 1.2 and 2.5. It was found that the pH of the bath and selenization process have a great influence on the structural, morphological, optical, compositional, and electrical properties of CIS film. The stoichiometric CIS thin films can be electrodeposited to lower cathodic potential for low pH of the bath, which could not only overcome the issues related to intense hydrogen evolution but also prevents the metallic elemental deposition. The compact and densely packed CIS thin films were deposited for both pH of the bath. Both as-deposited and selenized films showed tetragonal chalcopyrite structure with orientation along the (112) plane. The compressive strain was developed on the CIS films deposited for both pH values of the bath, which was further found to be increased after selenization and could be due to enhancement in the particle size as well as recrystallization of grains. The band gap of CIS film was found to be 1.03 to 1.06 eV for selenized CIS thin films obtained from the solution of pH 1.2 and 2.5, respectively. Electrical measurement showed Schottky behavior. The ideality factor (η) determined for the as-deposited and selenized films electrodeposited at −0.6 V in pH 1.2 bath were 1.6 and 1.3 and at −0.8 V in 2.5 pH bath were 1.9 and 1.2, respectively. The values of the ideality factor decreasing after selenization indicates the formation of ideal diode due to increase in shunt resistance. The photocurrent measured for selenized CIS thin films confirms the p-type conductivity under illumination of white light.

Acknowledgments The authors wish to acknowledge the finacial support from Defence Research and Development Organisation (DRDO), New Delhi under the major project grant ERIP/ER/10003866/M/01/1388.

References

1. Chaure NB, Young J, Samantilleke AP, Dharmadasa IM (2004) Sol Energy Mater Sol Cells 81:125–133
2. Jackson P, Hariskos D, Lotter E, Paetel S, Wuerz R, Menner R, Wischmann W, Powalla M (2011) Prog Photovolt Res Appl 19:894–897
3. Lakhe M, Chaure NB (2014) Sol Energy Mater Sol Cells 123:122–129
4. Moharram A, Hafiz MM, Salem A (2001) Appl Surf Sci 172:1–2
5. Repins IM, Contreras B, Egaas D, Scharf J, Perkins C, To B, Noufi R (2008) Prog Photovolt Res Appl 16:235–239
6. Terasako T, Uno Y, Kariya T (2006) Sol Energy Mater Sol Cells 90: 262–275
7. Niki S, Yamada A, Hunger R (2002) J Cryst Growth 237–239:1993–1999
8. Tiwari AN, Krejci M, Haug FJ, Zogg H (1999) Prog Photovolt Res Appl 7:393–397
9. Ashida A, Hachiuma Y, Yamamoyo N, Cho Y (1994) J Math Sci Lett 13:1181–1184
10. Wang XL, Wang GJ, Tian BL, Du ZL (2010) Chin Sci Bull 55:1854–1858
11. Lee H, Lee W, Kim J, Ko M, Kim K, Seo K, Lee D, Kim H (2013) Electrochim Acta 87:450–456
12. Chaure NB, Samantilleke AP, Burton RP, Young J, Dharmadasa IM (2005) Thin Solid Films 472:212–216
13. Yang J, Liu L, Li J, Liu Y (2012) Electrochem Solid State Lett 15: D19–D21
14. Padros A, Briones F, Sanz F (2010) Electrochem Commun 12:1025–1029
15. Dhanwate VN, Chaure NB (2012) Appl Nanosci 3:1–5
16. Maldes M, Vazquez M, Goossens A (2008) Electrochim Acta 54: 524–529
17. Schon JH, Alberts V, Bucher E (1999) Semicond Sci Technol 14: 657–659
18. Mandati S, Sarada BV, Dey SR, Joshi SV (2013) J Electrochem Soc 160:D173–D177
19. Bouraiou A, Aida MS, Meglali O, Attaf N (2011) Curr Appl Phys 11: 1173–1178
20. Calixto ME, Sebastian PJ, Bhattacharya RN, Noufi R (1999) Sol Energy Mater Sol Cells 59:75–84
21. Bao-Ping S, Shan P, Bin-Bin H, Guang-Hong Y, Shao-Ming W, Zu-Liang D (2013) J Inorg Mater 28:141–145
22. Harris TM, Wilson JL, Bleakley M (1999) J Electrochem Soc 146: 1461–1464
23. Pourbiax M (1966) Atlas of electrochemical equlibra. Pergamon Press, New York
24. Kemell M, Ritala M, Leskela M (2005) Crit Rev Solid State Mater Sci 30:1–31
25. Oda Y, Matsubayashi M, Minemoto T (2009) J Cryst Growth 311: 738–741
26. Culliti BD, Stock SR (2001) Elements of x-ray diffraction. NJ Prentice-Hall Inc., Englewood Cliff
27. Nawale S, Ravi V, Mulla IS (2009) Sensors Actuators B 139:466–170
28. Kulkurni SK (2007) Nanotechnology, principles and applications. Capital publishing Co., India
29. Gupta S, Patidar D, Saxena NS, Sharma K (2009) Chalcogenide Lett 6:723–731
30. Tung RT (1992) Phys Rev B 45:13509–13523